

## Magnetocaloric Effect in Uncoated $Gd_{55}Al_{20}Co_{25}$ Amorphous Wires

Dawei Xing<sup>a</sup>, Hongxian Shen<sup>a</sup>, Jingshun Liu<sup>b</sup>, Huan Wang<sup>c</sup>, Fuyang Cao<sup>a</sup>, Faxing Qin<sup>c</sup>,

Dongming Chen<sup>a</sup>, Yanfen Liu<sup>a</sup>, Jianfei Sun<sup>a\*</sup>

<sup>a</sup>School of Materials Science and Engineering, Harbin Institute of Technology,  
Harbin 150001, People's Republic of China

<sup>b</sup>School of Materials Science and Engineering, Inner Mongolia University of Technology,  
Hohhot 010051, People's Republic of China

<sup>c</sup>Institute for Composites Science and Innovation – InCSI, College of Materials Science  
and Engineering, Zhejiang University, Hangzhou 310027, China

Received: September 9, 2014; Revised: September 30, 2015

The  $Gd_{55}Al_{20}Co_{25}$  amorphous wires exhibit a relatively strong magnetocaloric effect (MCE). These melt-extracted amorphous wires display second-order magnetic transition (SOMT) and the value of maximal magnetic entropy ( $-\Delta S_m$ ) for the melt-extracted wires is calculated to be  $\sim 9.7 \text{ J} \cdot \text{kg}^{-1} \cdot \text{K}^{-1}$  around the Curie point ( $T_C$ ) of  $\sim 110 \text{ K}$  with applied field of 5 T. Moreover, the melt-extracted amorphous wires show a high refrigerating efficiency with a relatively large cooling power (RCP,  $\sim 804 \text{ J} \cdot \text{kg}^{-1}$ ) and refrigeration capacity (RC,  $\sim 580 \text{ J} \cdot \text{kg}^{-1}$ ) under an applied magnetic field of 5T due to the broad paramagnetic-ferromagnetic (PM-FM) region associated with amorphous alloys. These favorable properties make melt-extracted Gd-based amorphous wires to be the potential refrigerant for magnetic refrigeration (MR) of liquid oxygen.

**Keywords:** melt-extraction, amorphous microwires, magnetic entropy change, refrigerating efficiency

### 1. Introduction

Magnetic refrigeration (MR) based on the magnetocaloric effect (MCE) of refrigerant has attracted more increasing interests of international research communities for its high-efficiency, energy saving and the possibility for replacement of traditional vapor compression refrigerators used at room temperature<sup>1</sup>. The MCE and corresponding working temperature of the magnetic refrigerants are two key parameters in the MR applications. At the very low temperatures such as hydrogen and helium liquefaction range or even mK range, paramagnetic salts i.e.  $Dy_3Ga_3O_{12}$  and  $Gd_3Ga_3O_{12}$  have been used as refrigerants in MR<sup>[2]</sup>. Moreover, the series of refrigerants with first-order magnetic transition (FOMT) such as  $La(Fe,Si)^{[3]}$ ,  $Gd(GeSi)^{[4]}$  and  $MnFePAs^{[5]}$  alloys and with second-order magnetic transition (SOMT) e.g. pure  $Gd^{[6]}$ ,  $Gd$ -based<sup>[7]</sup> and  $Dy$ -based<sup>[8]</sup> alloys are developed for MR which applied in liquid nitrogen or room temperatures.

The Gd-based amorphous alloys possess more interesting characteristics in MR applications among these refrigerants mentioned above. Gd is a unique member of the lanthanide series with large magnetic moment and its ground-state electronic configuration is  $4f^7(5d_6s)^{[3-9]}$ . In contrast to other rare earth metals, Gd has no orbital momentum, leading to a relatively small magnetocrystalline anisotropy and a wide composition range which is possible by alloying predominantly magnetic 3d transition elements<sup>10</sup>. Gd-based amorphous magnetic refrigerants also show some advantages over the

crystalline materials due to their larger temperature range of paramagnetic-ferromagnetic (PM-FM) which leading to large relatively cooling power (RCP) and refrigeration capacity (RC). This characteristic renders the amorphous alloys as the attractive candidates for magnetic refrigerants although their entropy change is much lower than that of crystalline materials. Moreover, Gd-based amorphous materials display many excellent properties due to their unique long-range disorder structure, i.e. relatively higher electrical resistivity thus reducing eddy currents, higher corrosion resistance for absence of grain boundaries, higher cost effectiveness, more excellent softly magnetic properties and outstanding mechanical properties<sup>11</sup>.

In this paper, an improved rapid quenching method named melt-extraction technique is applied for fabricating Gd-based amorphous wires. In comparison with the conventional methods, the melt-extraction method has a larger cooling rate of  $\sim 10^5\text{--}10^6 \text{ K/s}^{[12]}$ , thus the melt-extracted amorphous wires exhibit higher degree of amorphization than the components of bulk metallic glasses (BMGs) or amorphous ribbons. A variety of amorphous wires with excellent giant magneto-impedance (GMI) effects<sup>13,14</sup> and mechanical properties<sup>15</sup> were fabricated with this method. Herein, the MCE properties of melt-extracted  $Gd_{55}Al_{20}Co_{25}$  (at%) amorphous microwires are systematically investigated and these results display the melt-extracted Gd-based amorphous wires as a great promising refrigerant for magnetic refrigeration (MR) applications in liquid oxygen range.

\*e-mail: jfsun\_hit@263.net, jfsun@hit.edu.cn

## 2. Experimental

An ingot with nominal composition of  $\text{Gd}_{55}\text{Al}_{20}\text{Co}_{25}$  was firstly prepared in argon atmosphere by arc melting and then suction casted into an alloy rod with diameter of  $\sim 10$  mm. The raw materials are high-pure Gd (99.50%), Al (99.99%) and Co (99.99%) crystals. Subsequently, the rod was re-melted in a boron nitride (BN) pot by electro-magnetic induction and the melt was extracted by a copper wheel with high-speed rotation. The specific processing parameters are as follows: 1) the diameter and knife-edge of copper wheel are 320 mm and  $60^\circ$ , respectively; 2) linear velocity of the copper wheel is fixed at around 30 m/s; 3) the feeding rate of the melt is fixed at  $20 \mu\text{m/s}$ .<sup>[12]</sup> The morphology of melt-extracted  $\text{Gd}_{55}\text{Al}_{20}\text{Co}_{25}$  amorphous microwires was observed on a field-emission scanning electron microscope (SEM-Helios Nanolab600i) at 20 kV. The phase structure information of these as-extracted wires was identified by X-ray diffraction (XRD) method and the pattern was obtained on a D/max-rb (Rigaku) with  $\text{Cu K}\alpha$  radiation at room temperature. The glass transition temperature ( $T_g$ ) and initial temperature of crystallization ( $T_{x1}$ ) of the as-extracted wires were confirmed by exploring the thermo analysis on a differential scanning calorimeter (DSC) with heating rate of 20 K/min. The magnetocaloric effect (MCE) of the Gd-based microwires was evaluated by measuring isothermal magnetizations ( $M$ - $H$ ) curves on a commercial magnetic property measurement system (SQUID-VSM) performed by Quantum Design, the external magnetic field change ( $\Delta H$ ) is 5 T and the temperature range is from 20 to 200 K which interval is 10 K while near  $T_c$  reduced to 5 K.

## 3. Results and Discussions

### 3.1. Structure characteristics

As shown in inset of Figure 1a, the  $\text{Gd}_{55}\text{Al}_{20}\text{Co}_{25}$  microwires fabricated by the melt-extraction method are of high quality for their smooth surfaces and uniform diameters from  $\sim 20$ - $30 \mu\text{m}$ . The micro-size of the wires means a large specific surface area which benefits the heat exchange in cooling system. As shown in Figure 1a, only a broad diffuse

peak appears at  $\sim 33^\circ$  in the XRD pattern, indicating the amorphous characteristic of these Gd-based microwires.

Further to explore the thermal stability and confirming the amorphous feature of melt-extracted microwires, differential scanning calorimeter (DSC) analysis is performed over a temperature range of 400-800 K. As shown in Figure 1b, the DSC curve has an obvious endothermic reaction peak appearing at  $\sim 585$  K (marked by green unidirectional arrow, defined as glass transition temperature ( $T_g$ )), then followed by several exothermic peaks owing to the crystallization of the amorphous phase. The result is consistent with that of BMGs, and the several endothermic peaks display a complex and multi-step crystallization of the wires during the heating process. The temperature of  $\sim 637$  K marked by purple unidirectional arrow is denoted as temperature or initial temperature of crystallization ( $T_{x1}$ ), then the temperature range of super-cooled liquid can be calculated by  $\Delta T_x = T_{x1} - T_g$  and the result is  $\sim 52$  K.

### 3.2. Magnetocaloric properties

The temperature dependence of magnetization ( $M$ - $T$ ) of the melt-extracted  $\text{Gd}_{55}\text{Al}_{20}\text{Co}_{25}$  microwires was therefore measured in the applied field of 200 Oe from 20 to 200 K, as illustrated in Figure 2a. It clearly shows the ferromagnetic-paramagnetic transition with the temperature increasing. The derivative of  $M$ - $T$  curve is shown in the inset of Figure 2a and the Curie temperature ( $T_c$ ) defined as the minimum value of  $dM/dT$ - $T$  curve is  $\sim 110$  K and marked in green arrow. For exploring the PM-FM transition of the as-extracted wires, the  $H/M$  ( $H=200$  Oe) ratio of the  $M$ - $T$  curve as a function of the temperature is calculated. As exhibited in Figure 2b, the  $\text{Gd}_{55}\text{Al}_{20}\text{Co}_{25}$  amorphous microwires obey the Curie-Weiss law above  $T_c$  and the predominant exchange interaction of the as-extracted wires is ferromagnetic below  $T_c$  owing to the positive paramagnetic Curie points<sup>16</sup>. The temperature data were fitted to the Curie-Weiss law and by this way, the Curie ( $C$ ) and Weiss ( $\theta_p$ ) constants are determined. As shown in Figure 2b, the values of  $C$  and  $\theta_p$  are calculated as  $\sim 5.07 \text{ emu}\cdot\text{K/mol}$  and  $\sim 121$  K, respectively. Furthermore, the effective magnetic moments ( $\mu_{\text{eff}}$ ) are calculated as  $\mu_{\text{eff}}=6.4 \mu_B$ . The large  $\mu_{\text{eff}}$

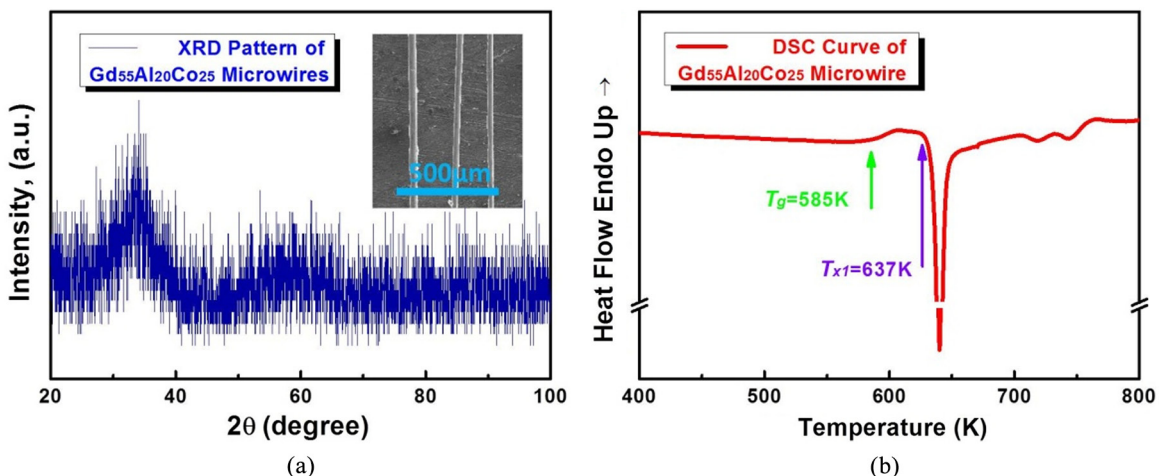


**Figure 1.** (a) XRD pattern and (b) DSC trace of melt-extracted  $\text{Gd}_{55}\text{Al}_{20}\text{Co}_{25}$  amorphous microwires, inset of (a) is the morphology of as-extracted wires.

is considered as the strong interaction of magnetic moment between transition metal (TM) element Co with 3d-electrons and rare-earth (RE) element Gd with 4f-electrons in the disordered amorphous wires, thus the excellent MCE of wires can be expected and obtained<sup>17</sup>.

Generally, the MCE is assessed by calculating the magnetization  $M$  as a function of the temperature  $T$  and the applied field  $H$ . Thus isothermal magnetization ( $M$ - $H$ ) curves of Gd<sub>55</sub>Al<sub>20</sub>Co<sub>25</sub> microwires at different temperatures of 20-200 K, which interval is 10 K while near  $T_c$  reduced to 5 K, were measured with the external magnetic fields up to 5 T ( $\Delta H=0$ -5 T) and the results are shown in inset of Figure 3a. To clarify the predominant exchange interactions of these microwires, the Arrott plots ( $H/M$  vs.  $M^2$ ) of the  $M$ - $H$  curves were calculated. As shown in Figure 3a, all the slopes of  $M^2$ - $H/M$  curves display positive values, also confirming that the PM-FM transition of these melt-extracted amorphous microwires is SOMT<sup>[18]</sup>. In addition, the  $M$ - $H$  loops of these microwires at 20 K were measured and shown in Figure 3b. The low coercivity ( $H_c \sim 30$  Oe) and remanence ( $M_r \sim 7$  emu/g) indicate a soft ferromagnetic

characteristic of these wires which is favorable for MR applications. Furthermore,  $M$ - $H$  loop at 20 K also exhibits small anisotropic field and large saturation magnetization ( $M_s$ ), combined with the characteristics of negligible thermal hysteresis and reduced magnetic hysteresis for SOMT materials, suggesting that low magnetic fields would lead to a large magnetic entropy change ( $-\Delta S_m$ )<sup>[19]</sup>.

The magnetic entropy change ( $-\Delta S_m$ ) of the as-extracted wires is evaluated from  $M$ - $H$  curves as shown in inset of Figure 2a through Maxwell relationship<sup>1</sup> as follows:

$$\Delta S_m(T, \Delta H) = S(T, H_2) - S(T, H_1) = \int_{H_1}^{H_2} \left( \frac{\partial M}{\partial T} \right)_H dH \quad (1)$$

And the result is calculated by a numerical approximation of the integral in Equation 1<sup>[20]</sup>:

$$-\Delta S_m(T_n) = \sum_i \frac{\Delta(M_{i+1} - M_i)}{\Delta(T_{n+1} - T_n)} \Delta H_i \quad (2)$$

where  $S$  is the magnetic entropy under given temperature  $T_n$ ,  $M_i$  and  $M_{i+1}$  represent the values of the magnetization at  $T_n$  and  $T_{n+1}$  under the applied field  $H_i$ , respectively.

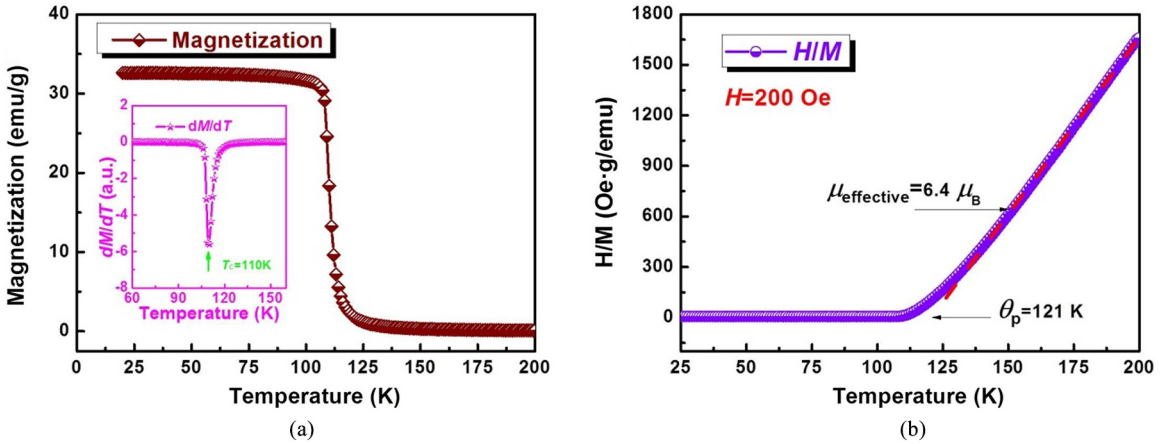


**Figure 2.** Magnetization as a function of temperature ( $M$ - $T$ ) from 20-200 K at applied field of 200 Oe for Gd<sub>55</sub>Al<sub>20</sub>Co<sub>25</sub> metallic glass microwires (a), the inset is the derivative result of  $M$ - $T$  curve, (b) the ratio of applied field  $H$  and magnetization  $M$  as a function of temperature result ( $H/M$ - $T$ ) of the wires.

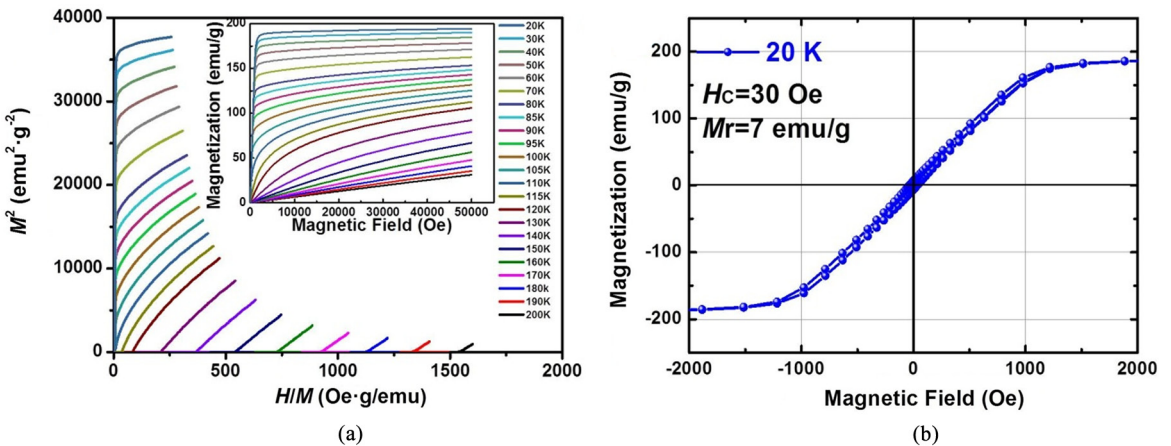


**Figure 3.** (a) Arrott plots ( $H/M$  vs.  $M^2$ ) of Gd<sub>55</sub>Al<sub>20</sub>Co<sub>25</sub> amorphous microwires constructed from isothermal magnetization ( $M$ - $H$ ) curves and the inset is the ( $M$ - $H$ ) curves at different selected temperatures from 20 K to 200 K with applied magnetic field of 0-5 T, (b) is the hysteresis loop ( $M$ - $H$ ) of the as-extracted microwires measured at 20 K.

The  $-\Delta S_m$  values of the melt-extracted  $Gd_{55}Al_{20}Co_{25}$  amorphous microwires at different temperatures from 25 to 195 K and under the varying applied magnetic field from 0 to 5 T are shown as three-dimensional (3D) image in Figure 4. It is well-known that the value of  $-\Delta S_m$  increases with the applied field increasing and maximum value ( $-\Delta S_m^{\max}$ ) reaches as large as  $\sim 9.7 \text{ J}\cdot\text{kg}^{-1}\cdot\text{K}^{-1}$  near the Curie temperature of  $\sim 110 \text{ K}$  under  $\Delta H=5 \text{ T}$ . This value is slightly larger than that ( $\sim 9 \text{ J}\cdot\text{kg}^{-1}\cdot\text{K}^{-1}$  at  $\sim 115 \text{ K}$ ) of its components in BMG<sup>[21]</sup> and almost similar to the value ( $\sim 9.7 \text{ J}\cdot\text{kg}^{-1}\cdot\text{K}^{-1}$  at  $\sim 100 \text{ K}$ ) of  $Gd_{55}Al_{25}Co_{20}$  metallic glass fibers<sup>[22]</sup> at  $\Delta H=5 \text{ T}$ , which suggests the excellent magnetocaloric properties of melt-extracted  $Gd_{55}Al_{20}Co_{25}$  amorphous microwires. But the result is smaller than that of  $Gd_{53}Al_{24}Co_{20}Zr_3$  amorphous wires ( $\sim 10.3 \text{ J}\cdot\text{kg}^{-1}\cdot\text{K}^{-1}$  at  $\sim 94 \text{ K}$ )<sup>6</sup>.

For understanding the MCE response to the magnetic field of the studied wires at Curie temperature, the peak entropy change  $-\Delta S_m^{\max}$  at applied field  $H$  was plotted in Figure 5a and followed the relationship for SOMT materials<sup>[23]</sup>:

$$-\Delta S_m^{\max} \propto H^n \quad (3)$$

The fitting curve of  $-\Delta S_m^{\max}$  points was plotted dash line in Figure 5a and leads to  $n=0.718$ , which is slightly lower than  $\sim 0.74$  of  $Gd_{53}Al_{24}Co_{20}Zr_3$  amorphous microwires<sup>[24]</sup>

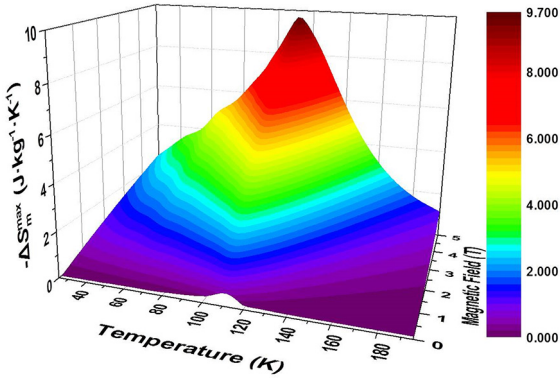
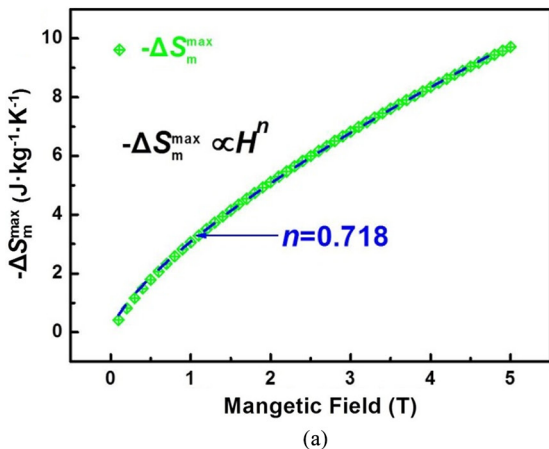
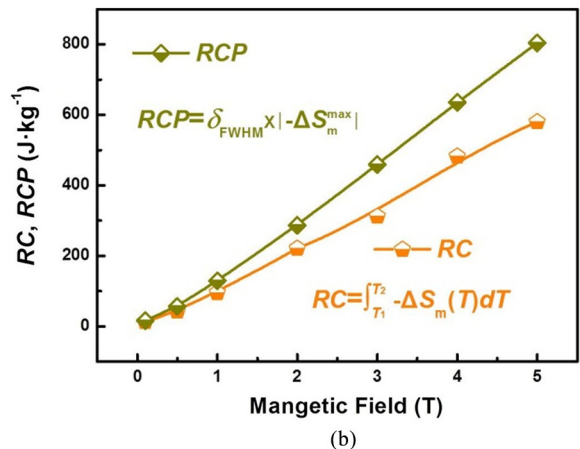


**Figure 4.** Magnetic entropy ( $-\Delta S_m$ ) values of melt-extracted  $Gd_{55}Al_{20}Co_{25}$  amorphous microwires at the temperature from 25 to 195 K under the varying applied magnetic field from 0 to 5 T.



(a)



(b)

**Figure 5.** (a) Peak entropy change  $-\Delta S_m^{\max}$  and b) RC, RCP values at different external magnetic fields  $\Delta H$  of melt-extracted  $Gd_{55}Al_{20}Co_{25}$  amorphous microwires.

and  $\sim 0.738$  of  $Gd_{55}Al_{25}Co_{20}$  metallic glass microfibers<sup>[22]</sup>. Commonly, the value  $n$  is  $2/3$  ( $\sim 0.667$ ) corresponding to mean field theory<sup>[25]</sup>, the deviation of the value for the studied wires is considered resulting from the inhomogeneous distribution on the amorphous matrix of nano-crystals in these wires. These nano-crystals formed during the melt-extracted process were considered for improving magnetic and mechanical properties of the amorphous alloys<sup>[15]</sup>.

The relatively cooling power (RCP) of the melt-extracted  $Gd_{55}Al_{20}Co_{25}$  amorphous microwires was calculated by the product between  $-\Delta S_m^{\max}$  and full width at half-maximum of the calculated  $-\Delta S_m$  peak ( $\delta_{FWHM}$ ):

$$RCP = -\Delta S_m^{\max} \times \delta_{FWHM} = -\Delta S_m^{\max} \times (T_2 - T_1) \quad (4)$$

where  $T_1$  and  $T_2$  are the onset and offset temperatures of  $\delta_{FWHM}$  and the related results are shown in Figure 5b. The  $\delta_{FWHM}$  and maximal RCP value are 83 K and  $\sim 804 \text{ J}\cdot\text{kg}^{-1}$  respectively at  $\Delta H=5 \text{ T}$ . The value is larger than that ( $\sim 800 \text{ J}\cdot\text{kg}^{-1}$ ) of its component in BMG<sup>[21]</sup>. Cooling efficiency of the studied wires is also evaluated by using refrigeration capacity (RC):

$$RC = \int_{T_1}^{T_2} -\Delta S_m(T) dT \quad (5)$$

where  $T_1$  and  $T_2$  are same as those in Equation 4, and generally RC is  $\sim 3/4$  of RCP<sup>[24]</sup> due to the broad triangular shape of  $-\Delta S_m$  vs.  $T$  peaks in these amorphous wires. The calculated results were also displayed in Figure 5b and for  $\Delta H=5 \text{ T}$ , the RC of studied wires is  $\sim 580 \text{ J}\cdot\text{kg}^{-1}$ , and this result is large than that ( $541 \text{ J}\cdot\text{kg}^{-1}$ ) of  $Gd_{55}Al_{25}Co_{20}$  BMG<sup>[20]</sup>, but less than that ( $652 \text{ J}\cdot\text{kg}^{-1}$ ) of  $Gd_{55}Al_{25}Co_{20}$  metallic glass fibers<sup>[22]</sup>. Thus, the large RCP and RC values display the excellent cooling efficiency and MCE of  $Gd_{55}Al_{20}Co_{25}$  amorphous microwires.

The large degree of amorphization due to the large cooling speed during the melt-extracted process and shape effect of the wires are considered for resulting in the excellent MCE of these Gd-base wires. As well-known, the long-range disorder microstructure of the amorphous alloys results in the fluctuation of exchange integrals, thus leading to broaden the PM-FM region of magnetic transition

in the amorphous wires<sup>26</sup>. In addition, when the axis of all measured melt-extracted Gd-based microwires are arranged parallel to the magnetic field direction, the demagnetizing factor ( $N$ ) is determined to be  $\sim 0$  due to the shape effect. Compared with its component in BMG or ribbon shape with  $n > 0$ , the  $-\Delta S_m$  increased significantly when temperatures are below  $T_c$ , while the  $-\Delta S_m$  almost remained unchanged as temperatures above  $T_c$ <sup>[27]</sup>.

## 4. Conclusions

Gd<sub>55</sub>Al<sub>20</sub>Co<sub>25</sub> amorphous microwires with excellent magnetocaloric effect were fabricated by a melt-extraction method with high quenching speed ( $\sim 10^6$  K/s). The predominant exchange interaction of as-extracted wires is SOMT around Curie temperature and the  $-\Delta S_m^{\max}$  is calculated to be  $\sim 9.7$  J·kg<sup>-1</sup>·K<sup>-1</sup> at  $\sim 110$  K as  $\Delta H = 5$  T. The RCP and RC of the wires are  $\sim 804$  J·kg<sup>-1</sup> and  $\sim 580$  J·kg<sup>-1</sup> respectively

when  $\Delta H = 5$  T. The excellent MCE of the melt-extracted Gd<sub>55</sub>Al<sub>20</sub>Co<sub>25</sub> amorphous microwires is considered due to the high degree of amorphization and their size effect.

## Acknowledgements

Dawei Xing acknowledges the support from National Natural Science Foundation of China (NSFC) under grant Nos. 51371067 and Dr. Chen Peng in Heilongjiang University for sample measurements. Jingshun Liu acknowledges the financial support provided by the National Natural Science Foundation of China (NSFC) under grant Nos. 51401111 and 51561026, Natural Science Foundation of Inner Mongolia Autonomous Region of China under grant Nos. 2014BS0503, and Scientific Research Foundation of the Higher Education Institutions (SRFHEI) of Inner Mongolia Autonomous Region of China under grant Nos. NJZY14062.

## References

- Phan MH and Yu SC. Review of the magnetocaloric effect in manganite materials. *Journal of Magnetism and Magnetic Materials*. 2007; 308(2):325-340. <http://dx.doi.org/10.1016/j.jmmm.2006.07.025>.
- Chang J, Hui X, Xu ZY, Lu ZP and Chen GL. Ni-Gd-Al metallic glasses with large magnetocaloric effect. *Intermetallics*. 2010; 18(6):1132-1136. <http://dx.doi.org/10.1016/j.intermet.2010.02.015>.
- Dong JD, Yan AR and Liu J. Microstructure and magnetocaloric properties of melt-extracted La-Fe-Si microwires. *Journal of Magnetism and Magnetic Materials*. 2014; 357:73-76. <http://dx.doi.org/10.1016/j.jmmm.2014.01.031>.
- Giguère A, Foldeaki M, Ravi Gopal B, Chahine R, Bose TK, Frydman A, et al. Direct measurement of the "giant" adiabatic temperature change in Gd<sub>5</sub>Si<sub>2</sub>Ge<sub>2</sub>. *Physical Review Letters*. 1999; 83(11):4190-4192. <http://dx.doi.org/10.1103/PhysRevLett.83.2262>.
- Tegus O, Brück E, Buschow KHJ and Boer FRD. Transition-metal-based magnetic refrigerants for room-temperature applications. *Nature*. 2002; 415(6868):150-152. <http://dx.doi.org/10.1038/415150a>. PMID:11805828.
- Bingham NS, Wang H, Qin FX, Peng HX, Sun JF, Franco V, et al. Excellent magnetocaloric properties of melt-extracted gd-based amorphous microwires. *Applied Physics Letters*. 2012; 101(10):102407. <http://dx.doi.org/10.1063/1.4751038>.
- Liang L, Hui X and Chen GL. Thermal stability and magnetocaloric properties of GdDyAlCo bulk metallic glasses. *Materials Science and Engineering B*. 2008; 147(1):13-18. <http://dx.doi.org/10.1016/j.mseb.2007.10.017>.
- Liang L, Hui X, Zhang CM and Chen GL. A Dy-based bulk metallic glass with high thermal stability and excellent magnetocaloric properties. *Journal of Alloys and Compounds*. 2008; 463(1-2):30-33. <http://dx.doi.org/10.1016/j.jallcom.2007.09.041>.
- Ding M and Poon SJ. Tunable perpendicular magnetic anisotropy in gdfeco amorphous films. *Journal of Magnetism and Magnetic Materials*. 2013; 339:51-55. <http://dx.doi.org/10.1016/j.jmmm.2013.03.007>.
- Schwarz B, Podmilsak B, Mattern N and Eckert J. Magnetocaloric effect in gd-based Gd<sub>60</sub>Fe<sub>x</sub>Co<sub>30-x</sub>Al<sub>10</sub> metallic glasses. *Journal of Magnetism and Magnetic Materials*. 2010; 322(16):2298-2303. <http://dx.doi.org/10.1016/j.jmmm.2010.02.029>.
- Atalay S, Gencer H, Kaya AO, Kolat VS and Izgi T. Influence of Si substitution on the structural, magnetic and magnetocaloric properties of Gd<sub>35</sub>Co<sub>20</sub>Fe<sub>5</sub>Al<sub>20-x</sub>Si<sub>x</sub> Alloys. *Journal of Non-Crystalline Solids*. 2013; 365:99-104. <http://dx.doi.org/10.1016/j.jnoncrysol.2013.01.042>.
- Wang H, Xing DW, Wang XD and Sun JF. Fabrication and characterization of melt-extracted co-based amorphous wires. *Metallurgical and Materials Transactions. A, Physical Metallurgy and Materials Science*. 2010; 42(4):1103-1108. <http://dx.doi.org/10.1007/s11661-010-0459-0>.
- Wang H, Qin FX, Xing DW, Cao FY, Peng HX and Sun JF. Fabrication and characterization of nano/amorphous dual-phase finemet microwires. *Materials Science and Engineering B*. 2013; 178(20):1483-1490. <http://dx.doi.org/10.1016/j.mseb.2013.09.010>.
- Liu JS, Qin FX, Chen DM, Shen HX, Wang H, Xing DW, et al. Combined current-modulation annealing induced enhancement of giant magnetoimpedance effect of Co-rich amorphous microwires. *Journal of Applied Physics*. 2014; 115(17):17A326. <http://dx.doi.org/10.1063/1.4865460>.
- Wang H, Qin FX, Xing DW, Cao FY, Wang XD, Peng HX, et al. Relating residual stress and microstructure to mechanical and giant magneto-impedance properties in cold-drawn Co-based amorphous microwires. *Acta Materialia*. 2012; 60(15):5425-5436. <http://dx.doi.org/10.1016/j.actamat.2012.06.047>.
- Xu ZY, Hui X, Wang ER, Chang J and Chen GL. Gd-Dy-Al-Co bulk metallic glasses with large magnetic entropy change and refrigeration capacity. *Journal of Alloys and Compounds*. 2010; 504:S146-S149. <http://dx.doi.org/10.1016/j.jallcom.2010.03.012>.
- Ding D, Tang MB and Xia L. Excellent glass forming ability and refrigeration capacity of a Gd<sub>55</sub>Al<sub>18</sub>Ni<sub>25</sub>Sn<sub>2</sub> bulk metallic glass. *Journal of Alloys and Compounds*. 2013; 581:828-831. <http://dx.doi.org/10.1016/j.jallcom.2013.07.137>.
- Zhong XC, Tang PF, Liu ZW, Zeng DC, Zheng ZG, Yu HY, et al. Magnetic properties and large magnetocaloric effect in Gd-Ni Amorphous ribbons for magnetic refrigeration applications in intermediate temperature range. *Journal of Alloys and Compounds*. 2011; 509(24):6889-6892. <http://dx.doi.org/10.1016/j.jallcom.2011.03.173>.
- Zhong XC, Gao BB, Liu ZW, Zheng ZG and Zeng DC. Amorphous and crystallized (Gd<sub>4</sub>Co<sub>3</sub>)<sub>100-x</sub>B<sub>x</sub> alloys for magnetic refrigerants working in the vicinity of 200 K. *Journal of Alloys and Compounds*. 2013; 553:152-156. <http://dx.doi.org/10.1016/j.jallcom.2012.11.086>.
- Du J, Zheng Q, Li YB, Li D and Zhang ZD. Large magnetocaloric effect and enhanced magnetic refrigeration in ternary gd-based

- bulk metallic glasses. *Journal of Applied Physics*. 2008; 103(2):023918. <http://dx.doi.org/10.1063/1.2836956>.
21. Lu S, Tang MB and Xia L. Excellent magnetocaloric effect of a  $Gd_{55}Al_{20}Co_{25}$  bulk metallic glass. *Physica B, Condensed Matter*. 2011; 406(18):3398-3401. <http://dx.doi.org/10.1016/j.physb.2011.06.006>.
  22. Shen HX, Wang H, Liu JS, Xing DW, Qin FX, Cao FY, et al. Enhanced magnetocaloric and mechanical properties of melt-extracted  $Gd_{55}Al_{25}Co_{20}$  micro-fibers. *Journal of Alloys and Compounds*. 2014; 603:167-171. <http://dx.doi.org/10.1016/j.jallcom.2014.03.053>.
  23. Franco V and Conde A. Scaling laws for the magnetocaloric effect in second order phase transitions: from physics to applications for the characterization of materials. *International Journal of Refrigeration*. 2010; 33(3):465-473. <http://dx.doi.org/10.1016/j.ijrefrig.2009.12.019>.
  24. Qin FX, Bingham NS, Wang H, Peng HX, Sun JF, Franco V, et al. Mechanical and magnetocaloric properties of Gd-based amorphous microwires fabricated by melt-extraction. *Acta Materialia*. 2013; 61(4):1284-1293. <http://dx.doi.org/10.1016/j.actamat.2012.11.006>.
  25. Oesterreicher H and Parker FT. Magnetic cooling near curie temperatures above 300 K. *Journal of Applied Physics*. 1984; 55(12):4334. <http://dx.doi.org/10.1063/1.333046>.
  26. Liu XY, Barclay JA, Gopal RB, Földeáki M, Chahine R, Bose TK, et al. Thermomagnetic properties of amorphous rare-earth alloys with Fe, Ni, or Co. *Journal of Applied Physics*. 1996; 79(3):1630. <http://dx.doi.org/10.1063/1.361007>.
  27. Caballero-Flores R, Franco V, Conde A, Kiss LF. Influence of the demagnetizing field on the determination of the magnetocaloric effect from magnetization curves. *Journal of Applied Physics*. 2009; 105(7):07A919. <http://dx.doi.org/10.1063/1.3067463>.